Determination of activation parameters for dislocation formation from a surface in fcc metals by atomistic simulations

P. Hirel,* J. Godet, S. Brochard, L. Pizzagalli, and P. Beauchamp
Laboratoire PHYMAT, UMR 6630 CNRS, Université de Poitiers, Bvd M. & P. Curie, Boite Postale 30179 – 86962 Futuroscope Chasseneuil Cedex, France

(Received 25 April 2008; revised manuscript received 2 July 2008; published 12 August 2008)

Defects in free surfaces are expected to be seeds for the nucleation of dislocations, which is the likely way nanoscale materials suffer plastic deformation. The nucleation results in the competition between the image force attracting the dislocation to the surface and the applied strain. In this work, two methods based on molecular dynamics simulations using an embedded atom method (EAM) potential are used to determine the activation energy and the critical radius for the formation of dislocations from a surface defect in a typical fcc metal.

DOI: 10.1103/PhysRevB.78.064109 PACS number(s): 62.20.−x, 61.72.Lk, 82.20.Pm, 82.20.Wt

I. INTRODUCTION

When reaching nanoscale dimensions, the properties of materials may be dramatically altered, issuing a great challenge in terms of both physical description and technological applications. In particular, the presence of defects in low-dimensional materials may significantly modify their mechanical, electrical, and optical properties, what can result in a dramatic effect on the behavior of devices.[1] Therefore, a better understanding of the mechanisms leading to defects nucleation in these nanostructures is of prime importance. Contrary to bulk materials for which Frank-Read sources are usually involved in the occurrence of plasticity,[2] nanoscale materials are unlikely to activate these sources because of their reduced dimensions. It is assumed that plasticity is then initiated by the nucleation of dislocations from surfaces, interfaces, or grain boundaries. For example, the elementary mechanisms occurring in work hardening of nanograined materials often involve nucleation from grain boundaries.[3–6] The nucleation of dislocations from crack tips is assumed to play a major role in the brittle to ductile transition in semiconductors.[7–9] Finally, in epitaxially grown thin films, the strain induced by lattice mismatch can lead to the formation of dislocations at interfaces.[10–12]

In the case of free surfaces, defects such as steps, terraces, or hillocks, have been experimentally observed to be favored places for the formation of dislocations,[13] a likely explanation being that they can locally concentrate the strain. However, experiments can hardly provide information at the smallest scales involved in the very beginning of the dislocation nucleation. Therefore, a computational approach appears to be appropriate for a fine investigation of such an event. Theoretically, dislocations are usually described within the theory of elasticity,[2] where they are treated like singularities in a continuum. Within this framework, the formation of dislocation loops near a free surface or interface has been widely discussed,[14–18] providing evidence of a competition between loop expansion favoring the stress release and the attraction of the dislocation by the free surface. There are therefore a critical size and an energy barrier to overcome for the dislocation to propagate throughout the system. These saddle-point parameters are essential in thermally activated processes, and can be considered intrinsic since they do not depend on external factors beside the applied strain. Thus, their characterization is a first theoretical step to the determination of quantities that are observable in experiments, such as the nucleation stress, which depend on other factors such as temperature and strain rate.[19]

Previous investigations suggest that this critical size should be small, with a half-loop radius of the order of few nanometers.[15,17] The elastic theory is known to fail at such a scale,[2] when the dislocation core is very close to the surface. It is then advisable to use another approach for investigating this problem, atomistic simulations with semiempirical potentials being particularly well suited. Such methods grant access to the desired atomic details and allow the modeling of large systems. Yet the use of reliable potentials is required, ensuring that the nucleation event and the shape and core of dislocations can be accurately reproduced. Embedded atom method (EAM) potentials for face-centered cubic (fcc) metals are possible candidates, since they have been shown to meet these requirements.[20–22] Here we consider aluminum as a model material because it is ductile at low temperatures, involving low thermal activation energies.

Former simulations that have focused on bidimensional aluminum slabs[23] have confirmed that the stress concentration near surface steps facilitates the nucleation of dislocations from these sites, but due to reduced dimensions only the formation of straight dislocations was allowed. In this study, the very first stages of plasticity are investigated for tridimensional systems presenting surface steps, and at high temperatures, the purpose being to characterize the formation of dislocation half loops. First, a description of the plastic events obtained by molecular dynamics (MD) simulations is presented. Then, specific methods are proposed for characterizing the so-called saddle point, i.e., calculate the critical radius and the activation energy associated with the nucleation. Two methods based on MD simulations are discussed and a custom elastic model is developed for comparison.

II. METHODS

The model system is a fcc aluminum slab including two opposite steps in one surface (Fig. 1). Periodic boundary

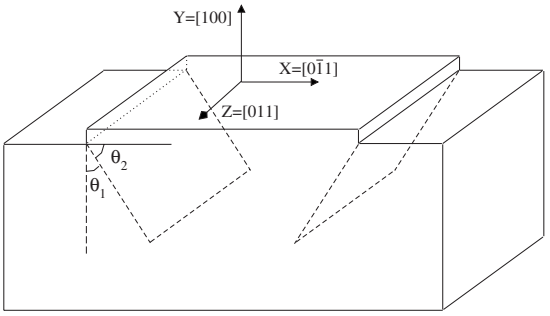

FIG. 1. Geometry of the system used in the simulations. The {111} glide planes passing through the step edges are drawn as thick dashed lines.

conditions are applied along the directions $X=[0\bar{1}1]$ and $Z=[011]$, while (100) surfaces remain free. The steps are built by adding a monoatomic layer in one surface. The steps line is orientated along Z, which is the intersection between a {111} plane, the primary glide plane in an fcc structure and the free surface. The crystal size used in this study is $170.55\times84.42\times170.55$ Å (142 800 atoms), and due to the periodic boundary conditions the smallest distance between the two steps is 56.85 Å. Simulations on larger crystals have shown that these dimensions are large enough to have a negligible influence on the presented results.

MD simulations are performed with the XMD code,[24] using a time step equal to 4×10^{-15} s, small enough to produce no energy drift during a 300 K run. Interactions between atoms are described by the EAM potential for aluminum proposed by Aslanides and Pontikis,[25] fitted on experimental values of cohesive energy, elastic moduli, vacancy formation, and intrinsic stacking fault energies, and known to reproduce correctly the dislocation core structures.[20] A temperature is introduced by assigning an initial Maxwell-Boltzmann distribution of velocities to the atoms and maintained by a smooth rescaling at each MD step. The strain is applied by elongating the simulation box along $X=[0\bar{1}1]$, i.e., orthogonally to the steps, and compressing it along the Y and Z axes, according to the Poisson's ratio of aluminum $\nu=0.35$, given by the EAM potential. The use of isotropic elasticity theory is justified by the low anisotropic character of this material,[26] and the applied strain and stress are considered linearly proportional, although it is not true at high applied strain.[27]

III. RESULTS

A. Formation of dislocation half loops

Tensile tests are performed with MD simulations as follows. The system is elongated up to 6%, with 1% increment every 5000 MD steps, i.e., every 20 ps. From then on, reduced increments are used, 0.1% every 5000 MD steps, corresponding to a strain rate of 5×10^7 s^{-1}. Figure 2 shows the typical outcome of a simulation at 100 K as the applied strain reaches 6.6%. Several dislocation embryos form on both steps, but quickly vanish, until one of them exceeds a critical radius and eventually expands in one of the two {111} planes passing through a step.

The occurrence of dislocation nucleation has been observed in all simulations performed at temperatures ranging from 80 to 300 K, for an applied strain about 6.5%–6.6%. This strain limit, although still relatively high, is greatly reduced compared to the case of a sample with no step (20%) and to a simulation performed at 0 K (10%), revealing the role of both the step and thermal activation in the initiation of plasticity. In addition, only straight dislocations were obtained at 0 K, showing that the nucleation of dislocation half loops requires thermal activation.[29] The formed defect is a Shockley partial, dragging a stacking fault. This is consistent with both the geometry of the system and the strain orientation, yielding the highest Schmid factor for Shockley partials.

B. Dislocation half-loop critical radius

In order to determine the critical size associated with the formation of a stable dislocation half loop for any applied strain, the following procedure has been used. During a MD run at 100 K and for an elongation $\epsilon=6.6\%$, atomic positions are saved every 50 steps, i.e., every 0.2 ps, as the dislocation half loop propagates through the crystal. Each of these configurations corresponds to a given dislocation half-loop radius R, which is here defined as the distance between the initial surface step and the dislocation front, and is determined by monitoring the relative displacements in {111} glide planes. Only half-loop sizes smaller than half the slab thickness have been selected in order to minimize the influence of the bottom surface. Each configuration is then brought to a lower applied strain, and atomic velocities are reset to zero in order to erase the system history. Our purpose is to determine, for the chosen applied strain, whether the

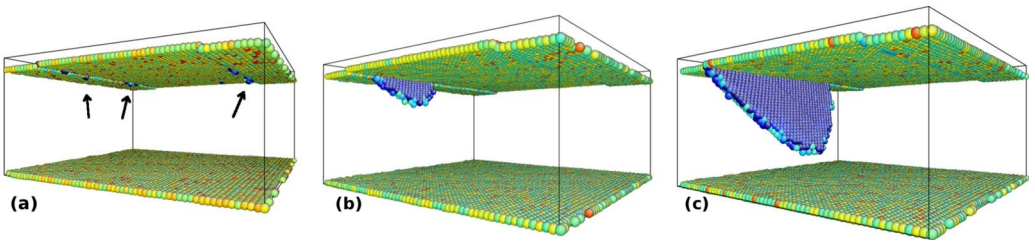

FIG. 2. (Color online) Evolution of a system under 6.6% applied strain at 100 K. Only atoms not in a perfect fcc environment are represented (Ref. 28) (a) Dislocation embryos appear randomly on both steps (arrows) and retract rapidly to the surface. (b),(c) Only when it reaches a critical radius will a dislocation half loop propagate into the crystal.

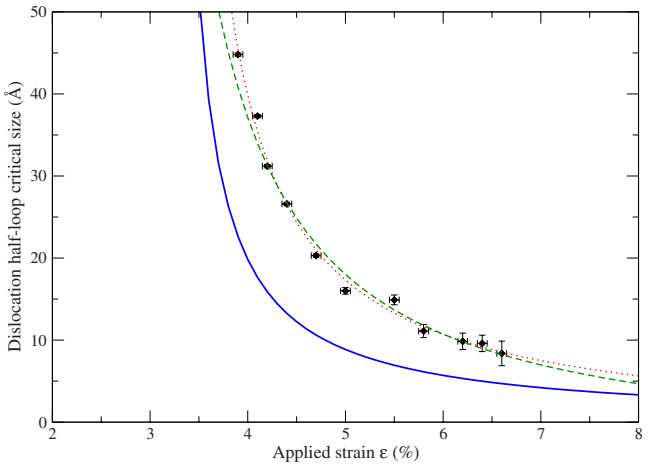

FIG. 3. (Color online) Critical radius R_c vs elongation obtained by MD (diamonds); the dotted line is a simple $1/\epsilon$ fit. The continuous line is the critical distance obtained from elasticity theory for a straight dislocation [Eq. (2)]; the dashed line is the one obtained from our fitted elastic model for an elliptic dislocation [Eq. (6)].

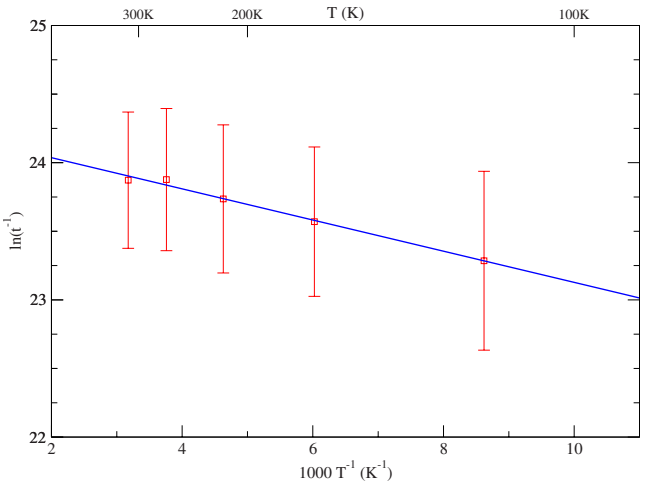

FIG. 4. (Color online) Arrhenius plot obtained from molecular dynamics and for several temperatures T ranging from 100 to 300 K for a sample elongated by ϵ=6.5%. t is the mean time required for a nucleation event to occur.

dislocation half loop will propagate into the crystal or will retract to the top surface, indicating that the initial radius R was larger or lower than the critical radius, respectively. At a given applied strain, systems with increasing dislocation sizes have been relaxed until a change in the dislocation propagation direction is observed, yielding the critical radius of the dislocation half loop.

This method has been performed for several elongations, thus providing the variation of the dislocation half-loop critical radius R_c versus the applied strain. The results of these simulations are shown as diamonds in Fig. 3. Our calculated R_c variation compares well to a fitted $1/\epsilon$ curve (dotted line), in agreement with the competition between two driving forces: the image force which roughly varies as $1/R$, and stress which is proportional to the applied strain ϵ. The critical radius becomes very small for high applied strains ($\epsilon > 6\%$), a radius that dislocation embryos may easily reach, meaning the nucleation becomes more probable. On the contrary, R_c dramatically increases as lower strains are applied, exceeding 40 Å for $\epsilon < 4\%$. So for low applied strains, the coherent motion of numerous atoms would be required to form and propagate a dislocation.

C. Determination of the activation energy

MD simulations also first appear as a good method to obtain the height of the energy barrier. Indeed, since the nucleation is a thermally activated event, the reaction rate theory[30] allows one to relate the nucleation time t to the temperature T and the activation energy E_a via an Arrhenius law:

$$t^{-1} = A \,.\, \exp\left(\frac{-E_a}{kT}\right), \tag{1}$$

where A is a temperature-independent factor, related to the nucleation attempt frequency and to the entropy of the system. It is then possible to determine E_a for a given applied strain by performing MD simulations at several temperatures.

Here, we have determined the activation energy for the nucleation of a dislocation half loop for an applied strain of 6.5%. For a given temperature in the range 100–300 K, the system is first thermalized at ϵ=6.4%. Then, the deformation is increased to 6.5%, this moment defining the origin of time, from which the time t until a nucleation event occurs is measured.

At least four simulations have been performed for each temperature, and the corresponding nucleation times averaged and drawn on an Arrhenius plot (Fig. 4). Error bars, corresponding to the standard deviation, are also drawn and shrink as the temperature increases. This is consistent with a thermally activated process: the higher the temperature, the lower the incertitude on the event time t. Finally, the activation energy for a strain ϵ=6.5% is estimated to be $E_a \approx 10$ meV.

D. Elastic model

Both the critical radius and the activation energy extracted from MD simulations can be compared to those obtained within the framework of elasticity. In the simplest case of a linear and isotropic model, one can first consider a straight dislocation emitted from a surface step in a continuous elastic medium. This dislocation is submitted to the glide force associated with the applied strain $F^{\epsilon} \propto \epsilon$, the so-called image force due to interaction with the free surface $F^{i} \propto 1/a$, with a being the dislocation-surface distance, and the force due to the stacking fault left behind the dislocation as it propagates, $F^{\mathrm{sf}} \propto \gamma$ with γ being the stacking fault energy per surface unit.[2] The critical dislocation distance a_c is reached when the total force on the dislocation vanishes, i.e., $F^{\epsilon} + F^{i} + F^{\mathrm{sf}} = 0$ projected in the glide plane, which gives

$$a_c = \frac{\mu b^2}{4\pi(1-\nu)(Eb\cos\,\theta_2\epsilon - \gamma)}, \tag{2}$$

where b is the Burgers vector associated with the dislocation, E and μ the Young and shear modulus of the material, re-

spectively, ν the Poisson's ratio, ϵ the applied strain, and θ_2 the angle between the Burgers vector of the dislocation and the direction of the applied strain (Fig. 1).

This critical distance a_c has been computed for different elongations, and plotted on Fig. 2 (solid line). It does not match the critical radius obtained from MD for a dislocation half loop, however it reproduces the trend that the critical radius increases very rapidly for low strains $\lesssim 4\%$.

A more realistic description can be built within the frame of elasticity. We consider here an elliptic dislocation half loop emerging from a surface step in a linear and isotropic medium. Such a dislocation is submitted to forces derived from several independent energy contributions: the dislocation self-energy, the dislocation-surface interaction, the relaxed strain energy, and the surface step and stacking fault energies.

The presence of a dislocation half loop of radius R increases the energy of the system by an energy E_d, including its self-energy and the interaction with the surface. To calculate this contribution, Beltz and Freund[15] have developed convincing arguments for using half the self-energy of a full circular dislocation loop in an infinite medium,[2] and for introducing a geometry-dependent factor m in this expression to take the interaction with the surface into account:

$$E_d = \frac{\mu b^2(2-\nu)}{8(1-\nu)} R\left[\ln\left(\frac{8m\alpha R}{b}\right) - 2\right], \tag{3}$$

where $\alpha = b/r_0$ is the dislocation core factor, r_0 being the core radius. In this model the authors derivate an expression for m that only depends on the material's Poisson ratio,[31] which leads to $m=0.554$, using the value of ν given by the EAM potential for aluminum used here. However, they considered a glide plane perpendicular to the surface, while in our system the glide plane is inclined. Also, our MD simulations show that dislocations are elliptic rather than circular. To take these effects into account, one can slightly adjust the value of m.

The strain energy E_ϵ relieved by the dislocation is expressed as

$$E_\epsilon = \frac{-\mu b(1+\nu)}{(1-\nu)} e\pi R^2 \cos\theta_1 \cos\theta_2 \epsilon, \tag{4}$$

where $\cos\theta_1 \cos\theta_2$ is the Schmid factor, with θ_1 being the angle between the normal to the surface and the direction of the Burgers vector (Fig. 1), and θ_2 the same angle as in Eq. (2). Here, we introduce an elliptic factor e, corresponding to the ratio between the two main axes of the elliptic dislocation (Fig. 5), so the surface covered by the elliptical dislocation half loop is $S=(\pi e R^2)/2$.

One also has to consider the shrinkage of the surface step. Here the step height is reduced by 2/3, corresponding to the projected norm of the Burgers vector, and over a distance equal to $2eR$. The associated relaxed energy can be expressed as $E_s = -(2/3)\times 2eR\sigma_S$, where $\sigma_S = 5.133 \times 10^{-11}$ J.m^{-1} is the energy per unit length of the surface step, calculated with the EAM potential used here.[32]

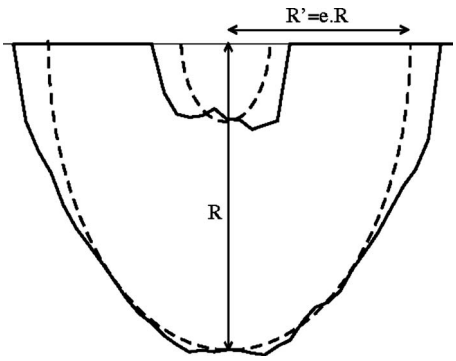

FIG. 5. Comparison between the dislocation shapes obtained by simulations (solid lines) and the elastic model proposed here (dashed lines) for two different radii.

Finally, the stacking fault dragged by the dislocation increases the system energy by a factor $E_\gamma = \gamma\pi e R^2/2$, where $\gamma = 0.155$ J.m^{-2} is the intrinsic stacking fault energy per surface unit in aluminum, provided by the EAM potential and in agreement with experimental data.[33,34] This energy is quite high and has a great influence on the results presented here.

Considering these terms, the variation of the total energy of the system due to a dislocation half loop propagating from a surface step is expressed as

$$E = E_d + E_\epsilon + E_s + E_\gamma. \tag{5}$$

The energy of the system is maximal when the dislocation half loop reaches the critical radius R_c, i.e., the saddle point defined by $dE/dR|_{R_c} = 0$ and $d^2E/dR^2|_{R_c} < 0$, insuring that the energy *decreases* as the dislocation radius increases. From this condition the following self-consistent equation for the critical half-loop radius is derived:

$$R_c = \frac{1}{16\pi e(1+\nu)\cos\theta_1 \cos\theta_2 \epsilon} \times \left\{ b(2-\nu)\left[\ln\left(\frac{8m\alpha R_c}{b}\right) - 1\right] + \frac{8e(1-\nu)}{\mu b}\left(\gamma\pi R_c - \frac{4}{3}\sigma_S\right)\right\}. \tag{6}$$

As expected, R_c is nearly inversely proportional to ϵ. Two parameters, $p=m\alpha$ and e, have to be adjusted on the critical radius curve described above (Fig. 3). Here we have considered $\alpha=2$, a typical value in fcc metals,[2] yielding $m=0.47$ and $e=0.82$, both values being consistent with the considerations assumed above. The R_c-strain curve obtained is reported on Fig. 3 (dashed line). The agreement with MD simulations is better than for a straight dislocation, however it shows slight deviations for both very large and very small radii.

These differences can be explained because our model is based on a perfect elliptic dislocation half loop with a constant ratio e between its main axes (Fig. 5), no matter the dislocation radius. On the contrary, analysis of the exact shape of the dislocations formed in the MD simulations shows that the ratio e decreases as the dislocation propa-

gates, i.e., the dislocation becomes more ellipsoidal when it goes deeper in the system; hence a model with a constant e cannot fit the dislocation shape for all radii. In addition, half loops obtained in simulations are not exactly half ellipses (Fig. 5). The elastic solution tends to underestimate the surface covered by the stacking fault, thus reducing its contribution to the total energy and underestimating the associated critical radius. The strain ϵ may also affect the dislocation shape since the force on the dislocation front will vary with ϵ but the force along the step will not; henceforth e may depend on both the dislocation radius R and the strain ϵ. Furthermore, the dislocation core becomes larger (hence α is smaller) when the dislocation approaches a surface. All these self-consistent dependencies make the problem almost intractable and have been ignored here. Another source of deviation is the bottom free surface, which attracts the dislocation in MD simulations and cannot be ignored for large radii.

IV. DISCUSSION

The efficiency of the Arrhenius method for determining the activation energy associated with the nucleation of a dislocation half loop is not obvious. Since it is stochastic, many MD simulations have to be performed, which makes it highly expensive in terms of computation time. In addition, for the strain discussed here, ϵ=6.5%, a wide range of nucleation times is obtained, leading to a great relative uncertainty in the activation energy. To improve the determination, the energy barrier would have to be chosen higher, i.e., lower strains have to be considered. However, for ϵ=6.5%, the nucleation time ranges from 40 to 200 ps, that is up to 50 000 MD steps, and the R_c-strain curve strongly suggests that for lower strains, the nucleation time will increase very rapidly. These considerations make difficult the use of such a method for low strains, hence it is not well suited for a systematic study of the activation energy at different applied strains.

Our developed elastic model provides analytical equations, granting access to the desired variations for any strain. It requires the fitting of two parameters, which was done here according to the critical radii obtained from MD simulations. One can then use elastic expression (5) to compute the variation of the energy as a dislocation half loop propagates into the system. This variation is represented in Fig. 6, for several strains, showing that both the activation energy and critical radius decrease as the applied strain increases. However, although expression (6) fits well the MD results, the activation energy obtained from the elastic model is far more sensitive to the fitted parameters. Hence complementary methods have to be used to calculate the activation energy for a large range of applied strains.

For instance, one could use a constrained relaxation method in order to obtain the energy of the saddle-point configuration, from which the activation energy can be extracted. Another well-suited method is the nudged elastic band (NEB) method,[35–37] which provides the full minimum energy path. The NEB method was already successfully used by Zhu *et al.*[9,19] to characterize the formation of dislocation half loops from crack tips[9] or from ledges in nanopillars,[19]

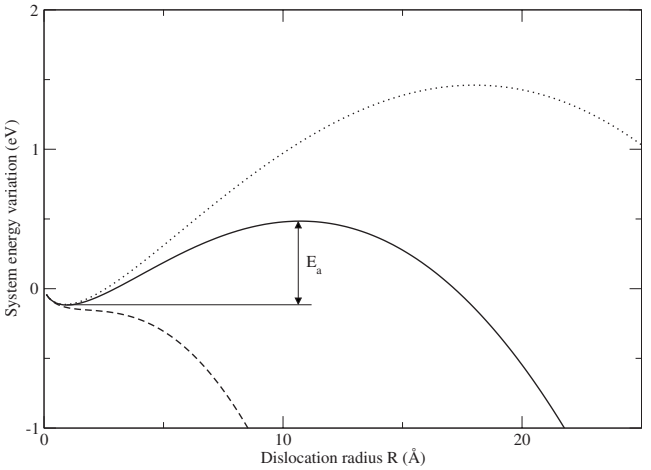

FIG. 6. Variation of the system energy vs the dislocation half-loop radius, calculated using the elastic model presented here for different applied strains: ϵ=5% (dotted line), 6% (continuous line), and 10% (dashed line). The so-called activation energy is represented.

and results similar to those presented here were obtained. From a crack tip, the activation energy for a load of 75% of the athermal threshold was estimated to be 1.1 eV. From a nanopillar corner, it was estimated to be about 0.1 eV for the same load. These results are slightly higher and lower, respectively, than the activation energy evaluated here from the elastic model. It suggests that the nature of preexisting defects has a strong influence on the nucleation process. In experiments, various defects may be present, such as higher steps or terraces, cracks, grain boundaries, dislocations, or point defects, all of them likely to shift the energy barrier and thus to change the nucleation stress.

The evolution of the activation energy versus the applied strain as provided by the elastic model [Eq. (5)] allows one to compute the activation volume, defined as the derivative of the activation energy with stress, i.e., $\Omega(\sigma)=-\partial E_a/\partial\sigma$. The variation of Ω as a function of strain is represented in Fig. 7. For an applied strain ϵ=9.3%, both the activation volume and energy vanish so the nucleation is certain to happen even at 0 K. This strain level defines the so-called athermal threshold,[38] and is consistent with the elastic limit obtained previously by energy minimization at 0 K, which was about 10%.[29] For ϵ ranging from about 3.2 to 9.3%, the nucleation can be considered a thermally activated process, with associated activation volumes lower than $10b^3$. For $\epsilon \lesssim 3.2\%$, both the activation energy and volume become too high for thermal activation to be observable in MD simulations. Therefore, since MD simulations are bound to typical times not much longer than a nanosecond, high applied strains have to be used to achieve and study nucleation. On the contrary, a typical experiment lasts longer than a second so nucleation may be observed for strains lower than 3.2%. Finally, for an elongation lower than about 2.5%, the activation volume reaches very high values ($\geq 1000\ b^3$), meaning that the nucleation becomes very unlikely.

The intrinsic parameters defining the saddle-point configuration can hardly be characterized in experiments, but they can be used to determine the nucleation stress, i.e., the

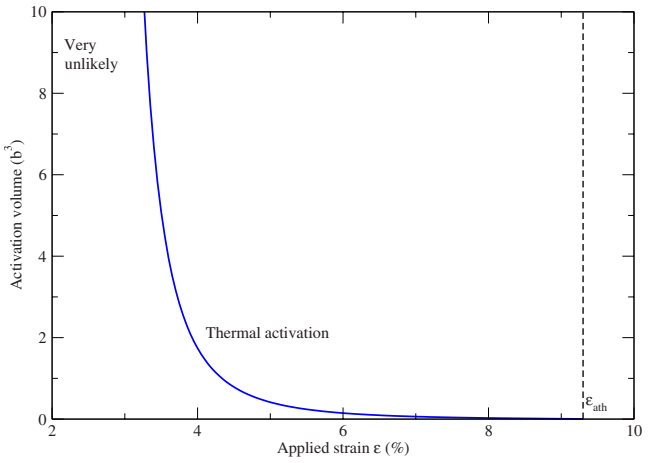

FIG. 7. (Color online) Activation volume as a function of the applied strain, calculated in the frame of the elastic model presented here.

stress at which one is likely to observe nucleation experimentally. This stress depends on temperature and strain rate $\dot{\epsilon}$, both quantities that can be varied in MD simulations. Nevertheless, strain rate in MD simulations can hardly be much lower than 10^7 s^{-1}, while it is typically less than 1 s^{-1} in experiments, which renders direct comparisons difficult. Using the saddle-point parameters, Zhu *et al.*[19] have shown that the nucleation stress can be reduced by almost a factor of two when comparing typical simulation strain rates ($\sim 10^8$ s^{-1}) to experimental ones ($\sim 10^{-3}$ s^{-1}), especially at high temperatures. Such a reduction should also occur for the mechanism studied here.

V. CONCLUSIONS

Molecular dynamics simulations using a semiempirical potential were used to characterize the activation parameters associated with the nucleation of a dislocation half loop from a surface step in an aluminum slab. The dislocation critical radius was calculated with a good accuracy and shown to increase very rapidly at low strains. The determination of the activation energy via Arrhenius plots revealed a poor efficiency, requiring high strains to keep reasonable simulation time and leading to great uncertainties. Other methods, such as the NEB method, shall be more appropriate to obtain the evolution of the energy barrier with strain. Such calculations are currently in progress to determine the activation energy in a complementary manner.

Using the theory of elasticity, we have improved an analytical model providing equations describing the forces and energy associated with a dislocation half loop in a semi-infinite medium. Our model, fitted on MD results, supposes that the nucleated dislocation has an elliptic shape. Using this model, it is confirmed that both the critical radius, activation energy, and volume rise to very high values at low strains.

ACKNOWLEDGMENTS

P. Hirel's Ph.D. work is supported by the Région Poitou-Charentes. We gratefully acknowledge the Agence Nationale de la Recherche for financing the project (No. ANR-06-blan-0250), and the IDRIS (Ref. 39) for providing computing resources.

*pierre.hirel@etu.univ-poitiers.fr

[1] E. Carrasco, O. R. de la Fuente, M. A. Gonzales, and J. M. Rojo, Eur. Phys. J. B **40**, 421 (2004).
[2] J. P. Hirth and J. Lothe, *Theory of Dislocations*, 2nd ed. (Krieger, Malabar, FL, 1982).
[3] D. E. Spearot, K. I. Jacob, and D. L. McDowell, Acta Mater. **53**, 3579 (2005).
[4] H. Van Swygenhoven, P. M. Derlet, and A. Hasnaoui, Phys. Rev. B **66**, 024101 (2002).
[5] V. Yamakov, D. Wolf, S. R. Phillpot, A. K. Mukherjee, and H. Gleiter, Nat. Mater. **1**, 45 (2002).
[6] V. Yamakov, D. Wolf, M. Salazar, S. R. Phillpot, and H. Gleiter, Acta Mater. **49**, 2713 (2001).
[7] F. Cleri, S. Yip, D. Wolf, and S. R. Phillpot, Phys. Rev. Lett. **79**, 1309 (1997).
[8] S. J. Zhou, D. M. Beazley, P. S. Lomdahl, and B. L. Holian, Phys. Rev. Lett. **78**, 479 (1997).
[9] T. Zhu, J. Li, and S. Yip, Phys. Rev. Lett. **93**, 025503 (2004).
[10] F. Ernst, Mater. Sci. Eng., A **233**, 126 (1997).
[11] O. Trushin, E. Granato, S. C. Ying, J. M. Kosterlitz, T. Ala-Nissila, and P. Salo, Braz. J. Phys. **32**, 369 (2002).
[12] X. Wu and G. Weatherly, Philos. Mag. A **81**, 1489 (2001).
[13] M. Albrecht, S. Christiansen, J. Michler, W. Dorsch, H. P. Strunk, P. O. Hansson, and E. Bauser, Appl. Phys. Lett. **67**, 1232 (1995).
[14] G. Xu and C. Zhang, J. Mech. Phys. Solids **51**, 1371 (2003).
[15] G. E. Beltz and L. B. Freund, Phys. Status Solidi A **180**, 303 (1993).
[16] J. P. Hirth, Acta Metall. Sin. (Engl. Lett.) **48**, 93 (2000).
[17] S. V. Kamat and J. P. Hirth, J. Appl. Phys. **67**, 6844 (1990).
[18] J. Zou and D. J. H. Cockayne, J. Appl. Phys. **79**, 7632 (1996).
[19] T. Zhu, J. Li, A. Samanta, A. Leach, and K. Gall, Phys. Rev. Lett. **100**, 025502 (2008).
[20] A. Aslanides and V. Pontikis, Comput. Mater. Sci. **10**, 401 (1998).
[21] M. S. Daw and M. I. Baskes, Phys. Rev. B **29**, 6443 (1984).
[22] S. M. Foiles, M. I. Baskes, and M. S. Daw, Phys. Rev. B **33**, 7983 (1986).
[23] S. Brochard, P. Beauchamp, and J. Grilhé, Phys. Rev. B **61**, 8707 (2000).
[24] J. Rifkin (http://xmd.sourceforge.net/).
[25] A. Aslanides and V. Pontikis, Philos. Mag. Lett. **78**, 377 (1998).
[26] Anisotropic coefficient of aluminum: $A=2C_{44}/(C_{11}-C_{12})=1.07$ (EAM potential used here); 1.22 (experiments Refs. 40 and 41).
[27] S. Brochard, P. Beauchamp, and J. Grilhé, Philos. Mag. A **80**, 503 (2000).

[28] J. Li, Modell. Simul. Mater. Sci. Eng. **11**, 173 (2003).
[29] P. Hirel, S. Brochard, L. Pizzagalli, and P. Beauchamp, Scr. Mater. **57**, 1141 (2007).
[30] P. Hanggi, P. Talkner, and M. Borkovec, Rev. Mod. Phys. **62**, 251 (1990).
[31] $m=\exp[(0.7734-1.059(2-\nu))/(2-\nu)]$.
[32] S. Brochard, P. Beauchamp, and J. Grilhé, Philos. Mag. Lett. **77**, 125 (1998).
[33] P. Coulomb, J. Microsc. Spectrosc. Electron. **3**, 295 (1978).
[34] M. J. Mills and P. Stadelmann, Philos. Mag. A **60**, 355 (1989).
[35] H. Jonsson, G. Mills, and K. Jacobsen, *Classical and Quantum Dynamics in Condensed Phase Simulations* (World Scientific, Singapore, 1998).
[36] G. Henkelman and H. Jonson, J. Chem. Phys. **113**, 9978 (2000).
[37] G. Henkelman, B. P. Uberuaga, and H. Jonsson, J. Chem. Phys. **113**, 9901 (2000).
[38] J. Li, MRS Bull. **32**, 151 (2007).
[39] Institut du Développement et des Ressources en Informatique Scientifique, http://www.idris.fr
[40] C. Zener, *Elasticity and Anelasticity of Metals* (University of Chicago, Chicago, 1948).
[41] J. F. Thomas, Phys. Rev. **175**, 955 (1968).